R. Justin Joseyphus
Jean-Marc Greneche

Fundamentals of ^{57}Fe Mössbauer Spectrometry

Springer

Fundamentals of ^{57}Fe Mössbauer Spectrometry

R. Justin Joseyphus · Jean-Marc Greneche

Fundamentals of ^{57}Fe Mössbauer Spectrometry

Springer

R. Justin Joseyphus
Department of Physics
National Institute of Technology
Tiruchirappalli, Tamil Nadu, India

Jean-Marc Greneche
Institut des Molécules et Matériaux du Mans
Le Mans Université-CNRS
Le Mans, France

ISBN 978-981-99-8652-1 ISBN 978-981-99-8653-8 (eBook)
https://doi.org/10.1007/978-981-99-8653-8

This Springer imprint is published by the registered company Springer Nature Singapore Pte Ltd.
The registered company address is: 152 Beach Road, #21-01/04 Gateway East, Singapore 189721, Singapore

Paper in this product is recyclable.

Preface

Rudolf Ludwig Mössbauer discovered the recoilless emission and resonant absorption of nuclear gamma rays due to his research work during the years 1955–58 at the Max Planck Institute in Heidelberg, Germany. The phenomenon is known as the Mössbauer effect, the spectrum as Mössbauer spectrum and the hyperfine parameters such as isomer shift, quadrupole splitting and hyperfine field as Mössbauer parameters. The Nobel Prize in Physics for 1961 was awarded to R. L. Mössbauer "for his researches concerning the resonance absorption of gamma radiation and his discovery in this connection of the effect which bears his name". The discovery stimulated interest and opportunities for further research in cross-disciplinary areas within a short period.

Mössbauer spectrometry is used across various disciplines such as Physics, Chemistry, Biology, Metallurgy, Materials and Geology, and this book is intended for a reader to know about a few important contributions in the relevant area. Chapters 1–3 of this book introduce the nucleus, quantum mechanics and magnetism. Readers familiar with these topics can revisit the concepts related to the Mössbauer effect. Chapters 4 and 5 deal with the fundamentals of the Mössbauer effect and Mössbauer parameters, respectively. Since the focus is on ^{57}Fe nucleus, the book covers the hyperfine parameters of important Fe compounds and their application in various disciplines related to materials, Earth, planetary and biological sciences, which are covered in Chaps. 6–13. The symbols and units used in the book have their usual meaning unless explicitly mentioned in each chapter.

R. Justin Joseyphus is thankful to Prof. A. Narayanasamy, who introduced him to the Mössbauer effect and experimental intricacies while he was at the University of Madras, Chennai, India. J.-M. Greneche is very grateful to Prof. F. Varret who, as his thesis supervisor, passed on to him his passion for research and the fundamentals of Mössbauer spectrometry, with great expertise in the theoretical and instrumental aspects and the numerical analysis of spectra, in correlation with the physical properties of the materials studied. He would also like to extend his warmest thanks to all the colleagues who, in the frame of various collaborative projects, have enabled him to successfully apply ^{57}Fe Mössbauer spectrometry to different types

of materials. The suggestions by Dr. J. Shebha Anandhi, Dr. R. Sankaranarayanan and Dr. R. Srinivasan are gratefully acknowledged.

The authors respect and recognize the contributions made by all the Mössbauer researchers worldwide. Nevertheless, suggestions, corrections and opinions are welcome that shall be acknowledged and incorporated in future editions.

Tiruchirappalli, India — R. Justin Joseyphus
Le Mans, France — Jean-Marc Greneche

Contents

Chapter 1
The Nucleus

1.1 Probing the Nucleus

Roentgen discovered X-rays in 1895, followed by the identification of other kinds of nuclear radiation in 1899 by Ernest Rutherford, known as alpha and beta rays. Paul-Villard, in 1900, found another form of radiation characterized by more penetration depth than X-rays and unaffected by electric or magnetic fields, named later on by Rutherford as γ-rays. Scattering experiments are used to probe the size and shape of the nucleus that requires energy sources over a few hundred MeV and wavelengths of less than a fm. Rutherford's analysis of the scattering of α-particles with a thin gold foil established that the atom has a positively charged nucleus, overturning the plum pudding model of J. J. Thomson. Rutherford scattering uses α particles that are difficult to produce with high energy, and therefore, electrons are used in scattering experiments to determine the nuclear size precisely. The electrons interact with the nucleus through electromagnetic interaction subject to the diffraction limits, whereas strong interaction is limited to the nucleons, and weak interaction is negligible.

The diffraction condition is satisfied if the de Broglie wavelength of the electron is equal to the size of the nucleus. Diffraction can be of two forms; far-field, known as Fraunhofer diffraction, and near-field, known as Fresnel diffraction. When the electron's kinetic energy is increased significantly and made to scatter on a nucleus, it is called relativistic scattering. The scattering cross section is then given by the Mott formula, which includes the effect of magnetic moment and recoil. The classical Rutherford scattering uses non-relativistic scattering considering only charge, neglecting recoil and magnetic moment. At very low electron energies, when the wavelength is larger than the size of the object, the interaction can be point-like, neglecting the spin. These effects are used to establish the properties of the nucleus.

R. J. Joseyphus and J.-M. Greneche, *Fundamentals of ^{57}Fe Mössbauer Spectrometry*,
https://doi.org/10.1007/978-981-99-8653-8_1

1.2 Constituents of the Nucleus

The nucleus has protons and neutrons known as nucleons, which are further made of fundamental particles called quarks. The quark structure is responsible for the positive and neutral charge of the protons and neutrons, respectively. The fundamental particles under two major classifications, known as leptons and quarks, with their charges, are shown in Table 1.1. The leptons have a charge of either −1 or 0, while the charges of quarks are either +2/3 or −1/3, in multiples of elementary charge. All ordinary matter is made up of particles comprising the leptons and quarks, whereas antiparticles are known for their opposite charges to that of particles.

The proton comprises two up quarks and a down quark where each up quark has an associated charge of + 2/3, and the down quark has a charge of − 1/3, making a net charge of + 1. Neutron has two down quarks and one up quark, resulting in a neutral charge. The quark constituents of the proton and neutron with their electric charges and another quantum number (color charge) represented by red, blue and green are shown in Fig. 1.1. The combination of the three color charges for a free particle has to be zero. Despite the neutral electric charge of the neutron, the strong nuclear force between the neutron and proton keeps them together, and the nuclear charges are uniformly distributed.

An atomic nucleus with its constituent proton (Z) and neutron (N) numbers is represented as ${}^{A}_{Z}\mathrm{X}$, where A is the mass number that is the sum of Z and N. The hydrogen nucleus has just one proton, while isotopes such as deuterium and tritium have one and two neutrons, respectively.

1.2.1 Charge Distribution

The nuclear charge distribution from scattering experiments is given by

$$\rho(r) = \frac{\rho_{\mathrm{o}}}{1 + \exp\left(\frac{r-R}{t}\right)} \tag{1.1}$$

Table 1.1 The fundamental particles and their charges

Leptons			Quarks		
Particle	Name	Charge (e)	Particle	Name	Charge (e)
e^-	Electron	−1	u	up	+2/3
μ^-	Muon	−1	d	down	−1/3
τ^-	Tau	−1	c	charm	+2/3
ν_{e}	Electron neutrino	0	s	strange	−1/3
ν_{μ}	Muon neutrino	0	t	top	+2/3
ν_{τ}	Tau neutrino	0	b	bottom	−1/3

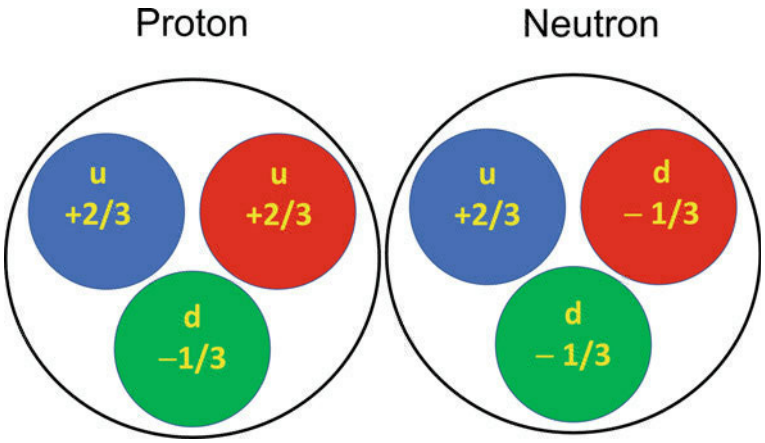

Fig. 1.1 The up (u) and down (d) quark constituents of the proton and neutron

In (1.1), ρ_o is the nuclear charge density near the nuclear core, R is the mean radius where the density decreases by half, and t is the skin thickness in which the density falls from 90 to 10%, as represented in Fig. 1.2. The density at the center of the nucleus is about $\rho_o = 0.16 \times 10^{45}$ nucleons/m^3. The radius of the nucleus is given by $R = 1.2A^{1/3} \times 10^{-15}$ m from electron scattering experiments. The nucleus can be approximated as a homogeneously charged sphere with a radius R. Another quantity often used is the mean square radius $<r^2>$ to take care of the not-so-well-defined radius and is related to R as

$$R^2 = \frac{5}{3}\langle r^2 \rangle \tag{1.2}$$

The root mean square (rms) radius of ^{56}Fe isotope is around 3.7 fm.

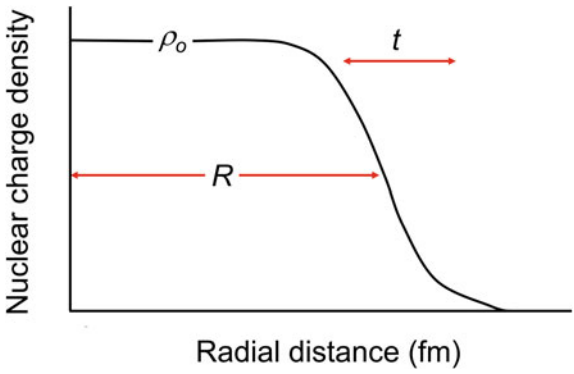

Fig. 1.2 The nuclear charge density variation with radial distance

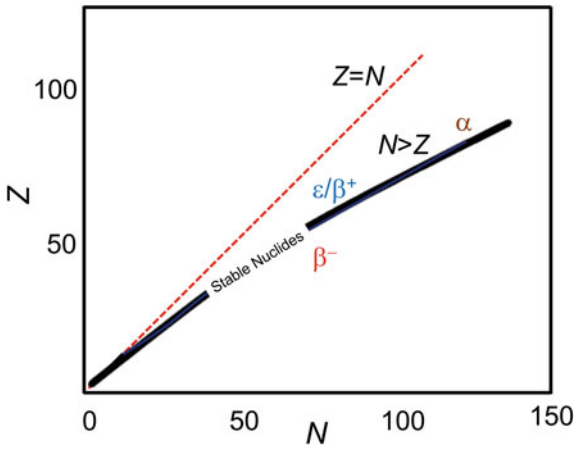

Fig. 1.3 Plot showing the deviation towards neutron-rich nuclei with higher mass numbers

As the number of protons in the nucleus increases, the number of neutrons must be added to overcome the Coulomb repulsion. The strong force thus holds the nucleons together, and as a result, most nuclei exhibit $N > Z$, as shown in Fig. 1.3. The stable nuclei are found in the valley of stability, while isotopes with excess protons and neutrons reach stability by moving towards the bottom of the valley. Those nuclei with excess protons beyond the stability line decay through β^+ or electron capture, whereas those with excess neutrons decay through β^-. The estimate of Coulomb energy for ^{56}Fe is

$$E_c = \frac{Ze^2}{4\pi\varepsilon_0 R} = \frac{Ze^2}{4\pi\varepsilon_0 R_o A^{1/3}} = \frac{26 \times (1.602 \times 10^{-19})^2}{4\pi\varepsilon_0 R_o \times 56^{1/3}} = 1.307 \times 10^{-12}\,\text{J} = 8.2\,\text{MeV}. \quad (1.3)$$

However, this estimate of the Coulomb energy term is modified inside a nucleus due to the contribution of more proton pairs. The e and ε_0 represent the elementary charge and vacuum permittivity, respectively.

As more neutrons are added up, the mass number increases and the nucleus becomes unstable. Nevertheless, a stable nucleus in most cases is due to another important factor, the binding energy.

1.3 Binding Energy

The sum of the individual nucleon's masses does not match the actual total mass of the nucleus, and this difference is known as the mass defect. The energy is being spent for binding nucleons together to achieve stability and hence known as binding energy given as

Table 1.2 Few of the isotopes of Fe and their relative abundance

Isotope	Z	N	Stability	Relative abundance (%)
^{52}Fe	26	26	Unstable—β^+ decay	–
^{54}Fe	26	28	Stable	5.8
^{55}Fe	26	29	Unstable—electron capture	–
^{56}Fe	26	30	Stable	91.8
^{57}Fe	26	31	Stable	2.1
^{58}Fe	26	32	Stable	0.3
^{59}Fe	26	33	Unstable—β^- decay	–

$$B = \left(\{Zm_{\mathrm{H}} + Nm_{\mathrm{n}}\} - m_Z^A\mathrm{X}\right)c^2 \tag{1.4}$$

where m_{H}, m_{n} and m are the masses of the hydrogen, neutron and atom, respectively, while electrons are also part of (1.4). The binding energy could be understood easily from the case of a deuteron. The deuteron is made up of a proton and a neutron. When a deuteron is formed, it releases a gamma ray of energy 2.2246 MeV equal to the binding energy. Similarly, the energy required to break the deuteron into proton and neutron is 2.2246 MeV.

1.4 Isotopes and Their Abundance

Nuclei with the same number of protons but with different neutron numbers are known as isotopes. Table 1.2 shows a few iron isotopes, their nucleon numbers and their stability. Stable isotopes such as ^{56}Fe and ^{57}Fe are relatively abundant, where the relative fractions are 91.8 and 2.1%, respectively (Meija et al. 2016). Here, the Fe isotopes can have either even or odd neutrons, one factor affecting their stability. The ^{56}Fe, ^{57}Fe and ^{58}Fe with $N = 30$, 31 and 32, respectively, lie at the bottom of the valley of stability. The Fe isotope with $N = 29$ decays through electron capture while $N < 28$ is by β^+ and $N > 33$ by means of β^- decay.

1.5 Binding Energy Per Nucleon

The stability of the isotopes is determined by the binding energy per nucleon, which is influenced by various contributions given in the semi-empirical mass formula. Derived by von Weizsäcker, on the analogy of liquid-drop, it assumes the nucleus is made of incompressible nuclear matter. The nuclear force is identical to each nucleon and saturates, implying that nearby nucleons only interact with each other. The total binding energy of the nucleus is a sum of various positive and negative contributions that are given by,

$$B = \text{volume term} - \text{surface term} - \text{Coulomb term} - \text{asymmetry term} + \text{pairing term}$$

The total binding energy is given by

$$B = a_v A - a_s A^{2/3} - a_c \frac{Z(Z-1)}{A^{1/3}} - a_a \frac{(A-2Z)^2}{A} + \delta \tag{1.5}$$

where a_v, a_s, a_c and a_a are constants.

The first term in (1.5), the volume term, is positive due to the attractive nuclear force, which is charge-independent. Since more nucleons imply a larger volume, the binding energy contributed by the volume term is,

$$B_{\mathrm{V}} \propto \frac{4}{3}\pi R^3 \propto A \tag{1.6}$$

The surface term contributes to a decrease in binding energy since

$$B_{\mathrm{S}} \propto 4\pi R^2 \propto A^{2/3} \tag{1.7}$$

The proton repulsion occurs in pairs which contribute to a term $Z(Z-1)$ and are included in the Coulomb energy contribution to the binding energy, assuming a uniformly charged sphere as

$$B_{\mathrm{C}} = \frac{3}{5}\frac{e^2}{4\pi\varepsilon_0 R} Z(Z-1) = \frac{3}{5}\frac{e^2}{4\pi\varepsilon_0 R_{\mathrm{o}} A^{1/3}} Z(Z-1) \tag{1.8}$$

A symmetrical number of protons and neutrons makes the nucleus more stable. To account for the binding energy contribution, the asymmetry term

$$\frac{(A-2Z)^2}{A} \tag{1.9}$$

has been introduced. An equal number of protons and neutrons eliminates the asymmetry term.

The pairing term was introduced to account for the binding energy contribution according to the odd or even nucleon contribution. If Z and N are even, then δ is positive, resulting in better stability of the nucleus. If Z and N are odd, the δ has a negative magnitude, and the term vanishes when $(N + Z)$ is odd. The various contributors to the binding energy with the mass number are shown in Fig. 1.4. The increase in the net *B/A* followed by the decrease at higher A is evident from the cumulative contributions.

The experimental binding energy per nucleon data for the nuclei, as shown in Fig. 1.5, could be fairly explained using the semi-empirical mass formula, although there are a few exceptions. The *B/A* curve results in better stability for $^4_2$He nucleus, which has even protons and even neutrons and also peaks around $A \approx 60$ that happens

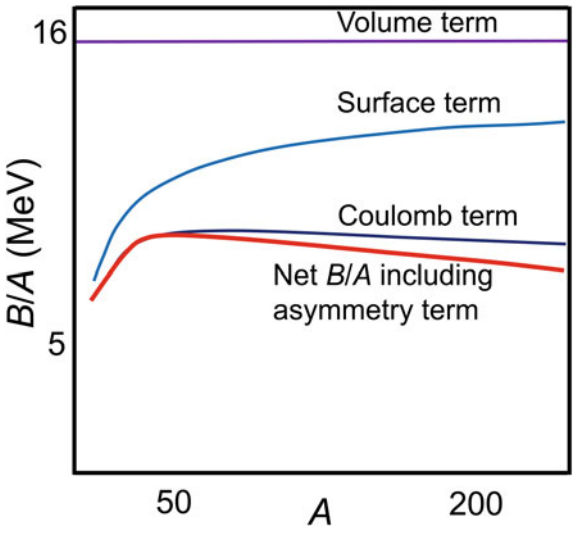

Fig. 1.4 Various cumulative contributions to the binding energy per nucleon (*B*/*A*) with mass number

to be the Fe and Ni nuclei. Thus, nuclei below $A \approx 60$ tend to fuse together and increase their *B/A,* whereas heavier nuclei try to shed their nucleons through the fission process.

The inset of Fig. 1.5 also shows the *B*/*A* values of a few isotopes that peak in the binding energy per nucleon curve (Fewell 1995). The largest *B*/*A* is for the ^{62}Ni isotope, while ^{56}Fe is the abundant isotope due to stellar nucleosynthesis.

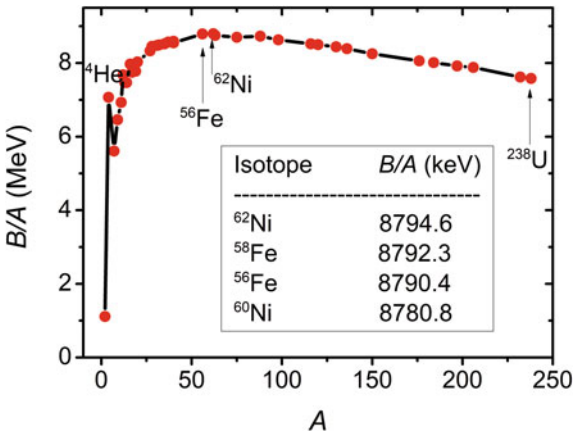

Fig. 1.5 The binding energy per nucleon (*B*/*A*) for a few isotopes with mass number. The *B*/*A* reaches a maximum at $A \approx 60$ and decreases for heavier isotopes such as ^{238}U

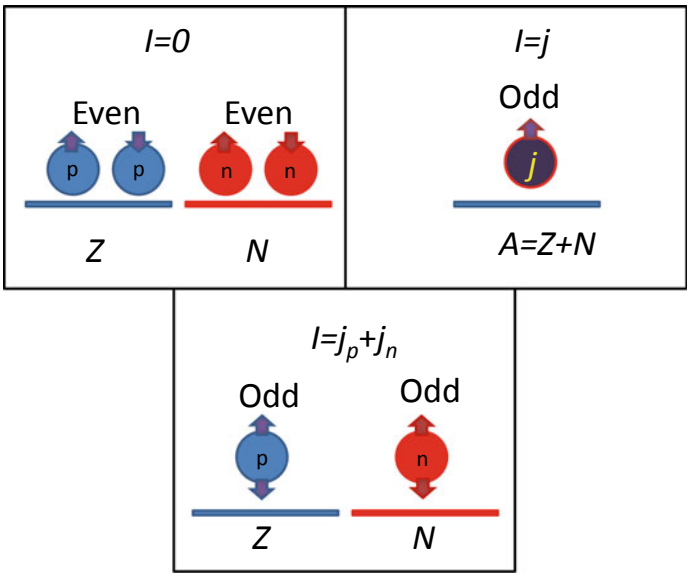

Fig. 1.6 The spin value of nuclei with even protons and neutrons is zero. The spin of the odd nucleon determines I for odd A and for nuclei with odd protons and odd neutrons

1.6 Nuclear Spin

The nuclear spin, I, is determined by the intrinsic orbital (l) and spin (s) angular momentum contribution of the nucleons (jj coupling) given as

$$I = \sum_{i=1}^{A}(l_i + s_i) = \sum_{i=1}^{A} j_i \tag{1.10}$$

The nuclear spin has a magnitude given by $\sqrt{I(I+1)}\hbar$ and its z component is $m_I\hbar$ where $m_I = +I,\ldots 0,\ldots -I$. The value of I could be obtained theoretically from nuclear models and in general, determined by the spin value of the odd nucleon as illustrated in Fig. 1.6. If: (i) Z and N are even, then $I = 0$; (ii) A is odd, I is determined by the j of the odd nucleon and; (iii) Z and N are odd, I is the sum of the spin values of the odd proton and neutron.

1.7 Nuclear Magnetic Moment

The magnetic moment of a nucleus is given by $\mu = gI\mu_N$, where g is the nuclear g-factor, I is the nuclear spin, and μ_N is the nuclear magneton. For the proton, the experimental spin g-factor is given by $g_p = 5.58569$,

whereas for the neutron, it is −3.82608. The experimental magnetic moment of a proton is +2.793 μ_N, while that of a neutron is −1.913 μ_N. These values are due to the quark-gluon constituents of the nucleons requiring relativistic treatment, or else the non-zero negative magnetic moment for the neutron would not be possible. For the ^{57}Fe isotope, the experimentally measured magnetic moment is + 0.0906 μ_N corresponding to $I = 1/2$ (Fuller 1976).

1.8 The Shell Model Nucleus

Certain nuclei with Z or N values 2, 8, 20, 28, 50, 82 and 126 are exceptionally stable, and these nucleon numbers are magic numbers. In the atomic case, the stability of atoms and the ionization energy can be explained by electrons in shells with definite energy levels. The energies of shells and subshells can be calculated using the Schrödinger equation and the Coulomb potential. However, for the nuclear case, a suitable potential has to be identified since the strong nuclear force influences the nucleons, and they move in a potential of other nucleons. A realistic model, which satisfies all the magic numbers given by Woods-Saxon mean field potential, is shown in Fig. 1.7.

Since the nuclear charge distribution varies at the boundaries of the nucleus, a gradually varying nuclear potential is a good approximation. The mean radius R, skin thickness, t are incorporated in the intermediate potential of the form known as Woods-Saxon potential given by

$$V(r) = -\frac{V_o}{1 + \exp\left(\frac{r-R}{t}\right)} \tag{1.11}$$

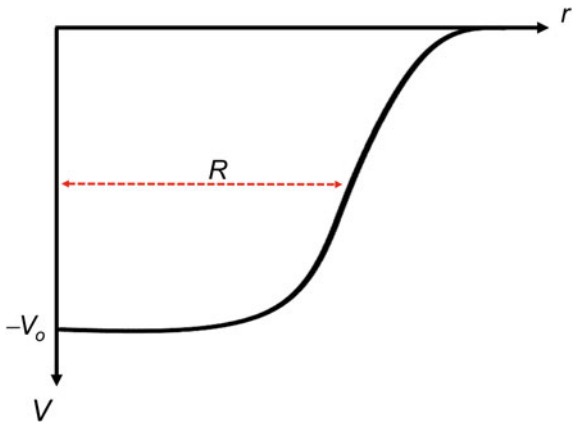

Fig. 1.7 The shell model Woods-Saxon mean field potential

where V_o is the depth of the potential well and r is the distance from the center of the nucleus. Solving the Schrödinger equation using (1.11) results in energy levels, as shown in Fig. 1.8.

The intermediate potential shown by the energy levels on the left side of Fig. 1.8 suggests magic numbers as 2, 8, 20, 40, 58 and 70, which does not satisfy the experimentally observed magic numbers. With the spin–orbit interaction term, fine

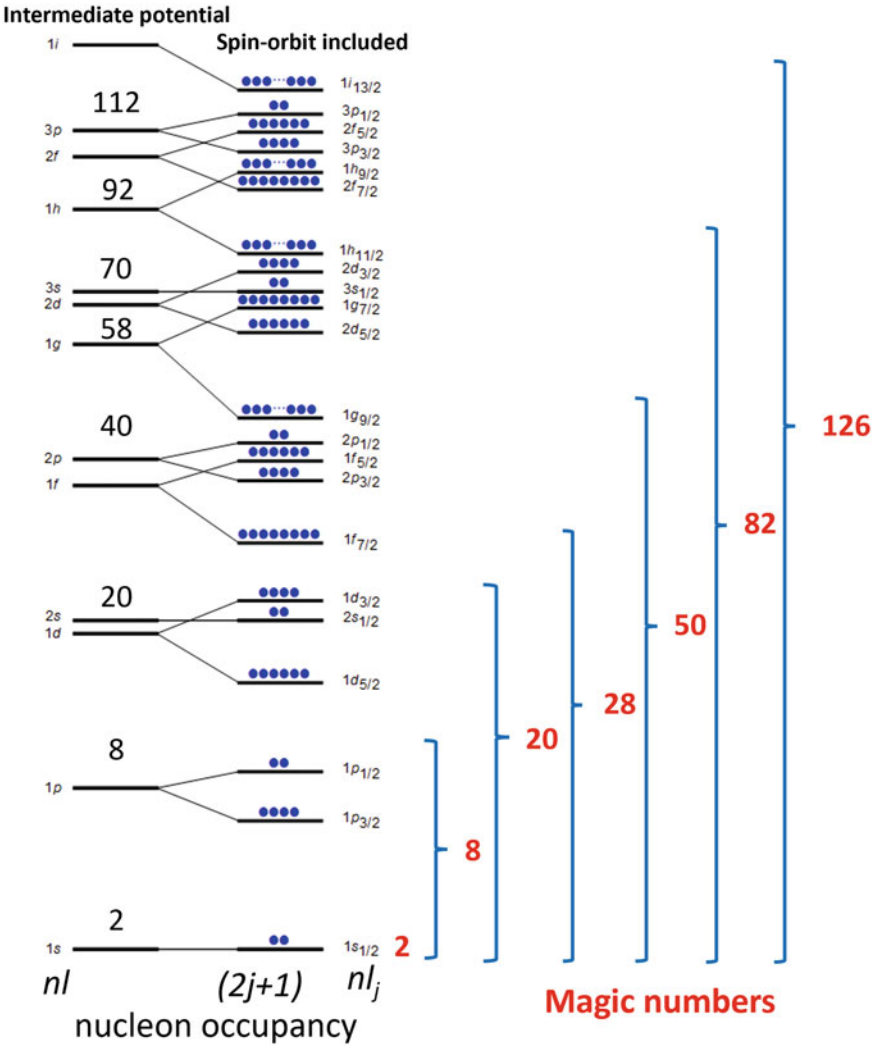

Fig. 1.8 The energy levels obtained using the intermediate potential (left) and the potential, including the spin–orbit term that satisfies all the magic numbers. The total nucleon occupancy in each level is given by $2j + 1$. Perturbations shift the energy levels. Simulated in Mathematica (Blinder 2009)

spectra were explained in atomic physics. A similar spin–orbit interaction term modifies (1.11) as $V_n(r) = V(r) + V_{ls}(r)$. Here, $V(r)$ is the Woods-Saxon and $V_{ls}(r)$ is the spin–orbit potential. The potential with spin–orbit term satisfies all the magic numbers and the energy levels as shown in Fig. 1.8. For example, the filling of energy levels corresponding to $1s_{1/2}$, $1p_{3/2}$, $1p_{1/2}$, $1d_{5/2}$, $2s_{1/2}$, $1d_{3/2}$, $1f_{7/2}$, $2p_{3/2}$, $1f_{5/2}$, $2p_{1/2}$ and $1g_{9/2}$ would satisfy the magic number 50. The occupancy of nucleons in each level is determined by the total angular momentum $j = l \pm s$. Thus, the $l = 0$ has only one $s_{1/2}$ level with an occupancy $2j + 1 = 2 \times 1/2 + 1 = 2$; $l = 1$ has levels $j = 1 + 1/2$ and $j = 1 - 1/2$ given as $p_{3/2}$ and $p_{1/2}$; $l = 2$ has levels $d_{5/2}$ and $d_{3/2}$ and so on.

Figure 1.9 shows the approximate proton and neutron potential where the nucleons are held together by the attractive strong force when $r < R$. For the proton, the Coulomb repulsion is included, which requires additional energy to overcome the barrier and get trapped in the potential well. The shell model also satisfactorily explains the spin and nuclear parity (π). All even-even nuclei have $j^\pi = 0^+$ ground states. For odd (A) nuclei, the unpaired nucleon determines the spin and parity given by j^π. Parity is given as $\pi = (-1)^l$. The spin and parity values for a few isotopes are shown in Table 1.3. The nuclei with even-even proton-neutron have zero spin, and the parity rule then gives a spin value of 0^+.

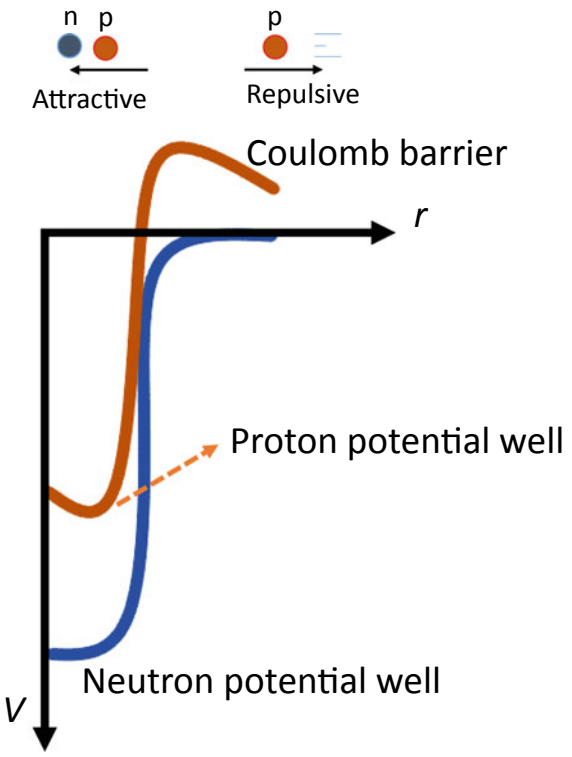

Fig. 1.9 The neutron potential well is only influenced by the strong force, whereas the strong force and Coulomb force determine the proton potential well

Table 1.3 The spin and parity values for a few Fe and Co isotopes

Isotope	N	j	Nucleons	Parity	Spin^{parity}
^{55}Fe	29	3/2	Even–odd	–	$3/2^-$
^{56}Fe	30	0	Even-even	+	0^+
^{57}Fe	31	1/2	Even–odd	–	$1/2^-$
^{58}Fe	32	0	Even-even	+	0^+
^{54}Co	27	0	Odd-odd	+	0^+
^{55}Co	28	7/2	Odd–even	–	$7/2^-$

1.9 Radioactive Decay

The number of nuclei $N(t)$ present at a given time (t) compared to the initial nuclei N_o ($t = 0$) is given by the radioactive decay law,

$$N(t) = N_o e^{-\lambda t} \tag{1.12}$$

where λ is the disintegration constant. As illustrated in Fig. 1.10, the initial nuclei N_o transform by radioactivity, and their number decreases exponentially with time as a function of λ, converting to another type of nuclei.

Half-life is the time required to reduce the number of nuclei to half its original value. Considering $N(t_{1/2}) = N_o/2$ and $t = t_{1/2}$ in (1.12) gives

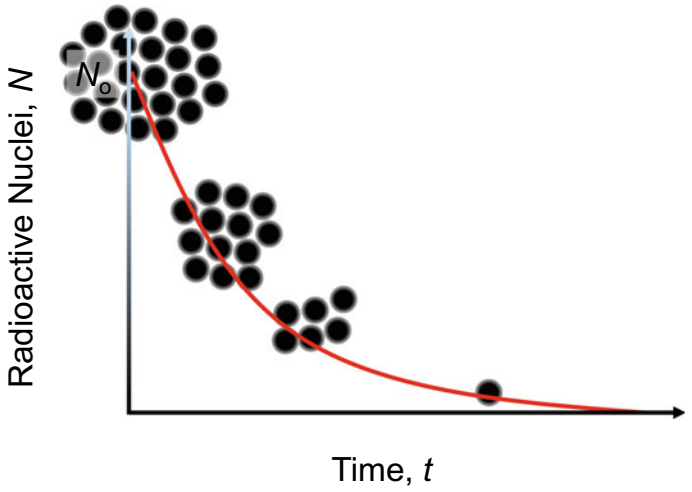

Fig. 1.10 The radioactive decay law is governed by the exponential decrease in nuclei from its initial number N_o over time, converting to another nuclei

$$t_{\frac{1}{2}} = \frac{0.693}{\lambda} \tag{1.13}$$

The mean-life is the average lifetime of nuclei given by

$$\tau = \frac{1}{\lambda} \tag{1.14}$$

The rate of radioactive decay is measured in terms of activity, which is the number of decays per unit time,

$$A = A_o e^{-\lambda t} \tag{1.15}$$

where $A_o = \lambda N_o$ is the activity at time $t = 0$. Activity is a measurable quantity in terms of cgs (centimetre–gram–second) unit curie (Ci) or in SI (Système International) unit as becquerel (Bq).

$$1\ \text{Ci}\ = 3.7 \times 10^{10}\ \text{decays/s}\ = 3.7 \times 10^{10}\ \text{Bq} = 37\ \text{GBq}.$$

Radioactive nuclei can decay using various routes giving different disintegration constants λ_1, λ_2, λ_3,… given as

$$N\left(\lambda_1 + \lambda_2 + \lambda_3 + \cdots\right) = N\lambda_t \tag{1.16}$$

The probability of various decay processes, when there is more than one, can be represented by branching ratios. ^{57}Co isotope is a category 5, low-risk source emitting gamma ray, used with a typical activity of 50 mCi.

Radioactive decay can be of three types (i) alpha (α) decay, (ii) beta (β) decay and (iii) gamma (γ) decay. The knocking out of a neutron or proton from the nucleus would also result in the transformation of the parent nucleus, accompanied by the emission of the above decay products. The α, β, and γ decays, as illustrated in Fig. 1.11, are due to quantum tunneling, weak interaction and deexcitation from higher to lower energies, respectively.

1.9.1 Alpha Decay

Alpha decay is the disintegration of the nucleus through the emission of $^4_2$He nucleus, known as α-particle. The disintegrating nucleus undergoes the following changes,

$${}^{A}_{Z}\mathrm{X}_N \rightarrow {}^{A-4}_{Z-2}\mathrm{X}'_{N-2} + {}^{4}_{2}\mathrm{He} \tag{1.17}$$

For the decay process (1.17), the conservation of energy implies the mass-energy and kinetic energy before disintegration should be equal to that after disintegration.

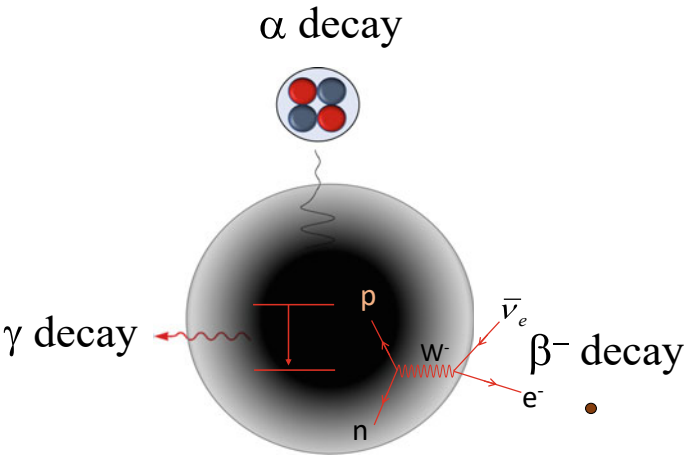

Fig. 1.11 The α-decay is due to quantum tunneling emitting positive charged $^4_2$He, β^- decay is a result of weak interaction, and γ-decay is caused by the transition in nuclear energy levels

The energy equation is written as

$$m_X c^2 + T_X = m_{X'} c^2 + T_{X'} + m_\alpha c^2 + T_\alpha \tag{1.18}$$

where c, m_X, T_X, $m_{X'}$, $T_{X'}$, m_α, T_α are the speed of light, mass of the initial nucleus, the kinetic energy of the initial nucleus, the mass of the final nucleus, the kinetic energy of the final nucleus, the mass of the alpha particle and the kinetic energy of the alpha particle, respectively. Assuming the initial nucleus is at rest, $T_X = 0$. Rearranging (1.18),

$$(m_X - m_{X'} - m_\alpha)c^2 = T_\alpha + T_{X'} = Q \tag{1.19}$$

The Q represented here is known as the Q-value, which is a measure of the energy released ($Q > 0$) or absorbed ($Q < 0$). A decay process will be spontaneous, provided $Q > 0$. From the conservation law, $T_\alpha + T_{X'} = Q$. Since the linear momentum of the initial nucleus is zero, the conservation of momentum gives

$$p_\alpha + p_{X'} = 0 \tag{1.20}$$

Therefore, the momenta of the α-particle and the final nucleus are equal and opposite. Note the recoil of the nucleus X′ coming into the picture here. We now obtain from (1.19),

$$T_\alpha \left(1 + \frac{T_{X'}}{T_\alpha}\right) = (m_X - m_{X'} - m_\alpha)c^2 = Q \tag{1.21}$$

Using the $T = p^2/2m$ relation, the kinetic energy of the alpha particle can be obtained as,

$$T_\alpha = \frac{Q}{\left(1 + \frac{T_{X'}}{T_\alpha}\right)} = \frac{Q}{\left(1 + \frac{m_\alpha}{m_{X'}}\right)} \tag{1.22}$$

Since $m_{X'} \gg m_\alpha$, $T_\alpha \approx Q$, implying that most of the Q value is contributed by the kinetic energy of the alpha particle. The Geiger-Nuttall law gives a typical Q value for α-particles in the range 4–10 MeV for half-life ranging from 10^{10} years to 10^{-7} s, respectively (Krane 1988). The Geiger-Nuttall law relates Q and half-life given as

$$\log t_{1/2} = a(Z) + \frac{b(Z)}{\sqrt{Q_\alpha}} \tag{1.23}$$

where a and b are functions of Z. This poses an important question. How could an alpha particle with energy as low as 4 MeV cross the nuclear potential barrier exceeding 8 MeV? This could be explained by quantum mechanics using the phenomena of barrier penetration or tunneling effect.

1.9.2 Beta Decay

The β-decay can take place through any of the following processes.

$$\begin{aligned} &\mathrm{n} \rightarrow \mathrm{p} + \mathrm{e}^- + \bar{\nu}_\mathrm{e} \quad \beta^- \text{ decay} \\ &\mathrm{p} \rightarrow \mathrm{n} + \mathrm{e}^+ + \nu_\mathrm{e} \quad \beta^+ \text{ decay} \\ &\mathrm{p} + \mathrm{e}^- \rightarrow \mathrm{n} + \nu_\mathrm{e} \quad \varepsilon \text{ electron capture} \end{aligned} \tag{1.24}$$

In the case of α-decay, the mass-energy of α-particle is 3.7 GeV, which is very large compared to the kinetic energy of 4 MeV and therefore, non-relativistic approach can be used there. Unlike α-particle, which has definite energy, experiments have shown that β-particle has continuous energy ranging up to a few MeV. It can be shown that the continuous distribution of kinetic energy is shared by the electron and neutrino in the β-decay process. The ^{22}Na isotope that decays to ^{22}Ne emitting e^+, with a half-life of 2.6 years, is widely used in positron annihilation spectroscopy.

The β^- decay transforms the nucleus as,

$${}^{A}_{Z}\mathrm{X}_N \rightarrow {}^{A}_{Z+1}\mathrm{X}'_{N-1} + \mathrm{e}^- + \bar{\nu}_\mathrm{e} \tag{1.25}$$

In terms of neutral atomic mass (M), nuclear mass (m) and electron mass (m_e), the mass-energy considering binding energy, is written as

$$M_X c^2 = m_X c^2 + Z m_e c^2 - \sum B \tag{1.26}$$

The antineutrino mass is negligible, electron masses and binding energies are eliminated here, and the Q value from (1.25) is

$$(M_X - M_{X'})c^2 = T_{e^-} + T_{\bar{\nu}_e} = Q \tag{1.27}$$

The β^- decay involves transforming higher to lower mass-energy due to the conversion of n $\rightarrow$ p that results in $Q > 0$. The electron and antineutrino share the kinetic energies. Let us not take this Q forward as we also define Q for nuclear quadrupole moment.

1.9.3 Gamma Decay

Any nuclear transition from a higher energy to a lower energy state involves the emission of high energy γ-ray photon. Unlike α and β decays, γ-decay does not involve any change in the nucleon number. The energies of γ-ray may overlap with the X-ray energy and the former is identified from its nuclear origin while the latter is related to the electron. Usually α and β decays produce isotopes in a higher energy state that reaches the ground state through the emission of γ-rays.

Consider a nucleus at rest emitting a γ-ray of energy E_γ after making a transition from excited state energy level, E_e to a lower level, E_g. Since the initial momentum is zero, the conservation of linear momentum should satisfy that the emitted gamma ray momentum is compensated with the recoil momentum giving

$$0 = p_R + p_\gamma \tag{1.28}$$

Using energy conservation,

$$E_e = E_g + E_\gamma + T_R \tag{1.29}$$

where T_R is the recoil energy.

Mössbauer spectroscopy deals with γ-rays, and therefore, it is important to know few of its characteristics. Unlike the α and β -rays, γ-ray has no definite absorption or penetration range because it is an electromagnetic radiation. The absorption of γ-rays of intensity I_o in a slab of thickness x can be given by the expression $I = I_o \exp(-\mu x)$ where μ is the absorption coefficient and I is the intensity after penetrating the slab. The thickness of the slab required to reduce the γ-ray intensity by half ($I/I_o = 1/2$) is known as *half-value thickness* or *half-value layer*. The absorption coefficient is proportional to the density of the material and microscopic cross section for reaction